

In-Band Distortion of Multisines

Khaled M. Gharaibeh, *Member, IEEE*, Kevin G. Gard, *Member, IEEE*, and Michael B. Steer, *Fellow, IEEE*

Abstract—Multisine signals are shown to be useful for estimating distortion of communication signals. In particular, a generalized approach for the evaluation of effective in-band distortion in a nonlinear amplifier using multisine excitation is presented. The output of the nonlinearity is represented as the sum of uncorrelated components by the transformation of a behavioral model. Simulated and measured results are presented for code-division multiple-access signals.

Index Terms—Intermodulation distortion, multisine signals, nonlinear distortion, nonlinear systems, signal analysis, signal representations.

I. INTRODUCTION

MULTISINE signals have been used to model the behavior of nonlinear systems because of the simplicity of the analysis and simulations. The design of multisines for modeling digitally modulated communication signals is usually based on the choice of the amplitudes, phases, and number of tones optimized for their suitability to capture adjacent channel power ratio (ACPR), in-band distortion, or other distortion metrics.

The rationale for using multisines is that they require lower computational complexity than that required by direct use of the actual communication signals. Multisine representations of signals have direct application in harmonic-balance simulation [1] and in measurement characterization of nonlinear microwave circuits [2]. Moreover, multisine analysis leads to an analytic evaluation of distortion with simple expressions for nonlinear system figures-of-merit such as intermodulation ratio (IMR), signal-to-noise ratio (SNR), ACPR, etc.

Transmitter signal quality in digital wireless communication systems is specified by the error vector magnitude (EVM) of the transmitted signal. EVM is inversely related to the signal-to-noise and distortion (SINAD) ratio, which measures the effective SNR including noise, distortion, and any other signals that degrade the effective SNR of the transmitter signal. There are many contributors to transmitter EVM degradation including thermal noise, phase noise, nonlinear distortion, spurious signals, etc. However, intermodulation distortion is a significant contributor to transmitter EVM degradation when operating at high output power levels in systems utilizing power efficient

nonlinear amplifiers. Here, the relationship between nonlinear transmitter distortion and transmitter SINAD degradation is investigated through analysis and measurements using multisine signals. In this context, we define effective in-band distortion as the component of the nonlinear output that shares the same frequency band as the input signal, but is “uncorrelated” with the ideal transmitter signal. From a communications point-of-view, the receiver is designed to distinguish between only two types of signals, which are: 1) the transmitted signal to which it is matched and 2) noise. Here, the term correlation refers not only to the statistical resemblance between the output and the input signals, but also to the ability of the receiver to recover useful information from the transmitter signal. Therefore, if part of the transmitted signal is uncorrelated with the expected waveform, that part of the signal is considered as uncorrelated distortion noise, which contributes to the degradation of transmitter SINAD.

The problem with characterizing effective in-band distortion is the identification of the effective terms of the nonlinear output that are responsible for in-band distortion inside the main band of the input signal spectrum. The reason for this is that the nonlinear output is partially correlated with the input signal, which subtracts or adds to the desired output signal causing gain compression or expansion. The remaining part of the nonlinear output is the uncorrelated in-band distortion noise, which may be treated as an additional contributor to in-band noise. Thus, both the correlated and uncorrelated components of the nonlinear output contribute to the degradation of system SINAD in different ways.

In [3], we presented an analysis of in-band distortion of multisines with random phases. In this paper, we provide an analytic approach to the identification of the effective in-band distortion of multisine signals using both deterministic and uniformly distributed random phases. We consider multisine signals with constant amplitudes and varying initial phases and derive the effective in-band distortion components. It is shown that the shape and level of the uncorrelated distortion spectrum depends on the initial phases, and this has different effects on in-band and out-of-band distortions. Estimated in-band distortion of multisine signals is verified by simulations and measured in-band distortion compared against an IS-95 forward-link code-division multiple-access (CDMA) signal using feed-forward cancellation. Multisine signals with 16 tones and random phase are shown to accurately predict the in-band distortion of a 64-user CDMA signal.

This paper is organized as follows. Section II is a review of the existing approaches to multisine analysis. Section III presents an analysis of in-band distortion of multisines with fixed initial phases. In Section IV, we present the probabilistic view of distortion where multisines have random phases. Section V presents simulation and measurement results of distortion in

Manuscript received December 15, 2005; revised May 12, 2006. This work was supported in part by the U.S. Army Research Office as a Multidisciplinary University Research Initiative on Multifunctional Adaptive Radio Radar and Sensors under Grant DAAD19-01-1-04 and under the William J. Pratt Assistant Professorship.

K. M. Gharaibeh is with the Hijjawi Faculty for Engineering Technology, Yarmouk University, Irbid 21163, Jordan (e-mail: kmgharai@ieee.org).

K. G. Gard and M. B. Steer are with the Electrical and Computer Engineering Department, North Carolina State University, Raleigh, NC 27695-7914 USA (e-mail: kggard@ncsu.edu).

Digital Object Identifier 10.1109/TMTT.2006.879170

multisine signals where we show how effective in-band distortion of a 64-user CDMA signal is estimated from that of multisines with random phases.

II. BACKGROUND

Considerable research has been undertaken on using multisine signals for characterizing distortion in nonlinear systems. Interest has grown with the introduction of large-signal vector network analyzers (VNAs), which use multisine inputs for device characterization. Remley [4] used multisine signals with random and deterministic amplitude and phase for ACPR simulation. It was demonstrated that certain choices either overestimate or underestimate ACPR of real communication signals. Pedro and de Carvalho [5]–[7] used multisine signals to simulate the spectrum of communication signals subject to a nonlinear system with memory. Optimization criteria were used to design multisine signals that mimic the spectral characteristics of communication signals. Although the analysis was based on Volterra series, a simplification of the Volterra model was used to perform simulations. Boulejfen *et al.* [8] considered the estimation of in-band and out-of-band distortions of communication signals using multisine signals with random phases. The approach was analytic and enabled ACPR, noise power ratio (NPR) and co-channel power ratio (CCPR) to be estimated for a fifth-order nonlinearity. However, it was not shown that the approach can truly represent the in-band distortion in real communication signals. In [9] and [10], the design of multisine signals for a minimal crest factor was studied. The analysis was useful for constructing test signals to measure the frequency response of linear systems. It is questionable, however, that this approach could be used for estimating nonlinear system distortion because of the low correlation between the crest factor and distortion [11]. Geens *et al.* [12] used multisines with random phases to estimate NPR and CCPR. They showed that NPR is not always a valid metric for in-band distortion.

A common characteristic of the above approaches is that they use the Gaussian approximation of multisine signals. The identification of the uncorrelated distortion noise is straightforward using the statistical properties of Gaussian processes. A theoretical analysis of the decomposition of the output spectrum into uncorrelated components without using the Gaussian assumption was studied in [13] and [14] where, based on the properties of the distribution function of the input signals, the output of a bandpass nonlinearity can be expressed as a sum of uncorrelated components.

An approach for the identification of the effective in-band distortion of CDMA signals without using the Gaussian assumption was presented by the authors in [15]. The approach was based on the orthogonalization of the behavioral model and leads to exact identification of effective in-band distortion. The approach was used to accurately estimate system metrics such as SNR, EVM, and ρ of CDMA signals. It is well established that the sum of a large number of sinusoids with random phases converges to a band-limited Gaussian noise process by the central limit theorem [2]. However, the approach is valid for any random process that satisfies the separability condition and,

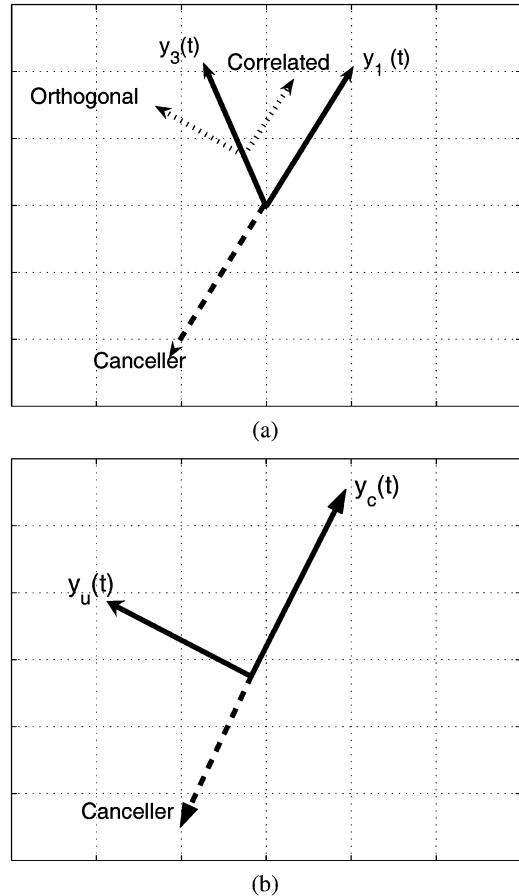


Fig. 1. Geometrical interpretation of in-band distortion. (a) Distortion vector. (b) Orthogonal representations.

hence, it can be used with a small number of tones, as will be shown here.

III. DISTORTION OF MULTISINES

Effective in-band distortion of multisines can be understood by defining the uncorrelated component of the nonlinear output. Considering a memoryless nonlinearity, a geometrical representation of the nonlinear output is shown in Fig. 1 where the total output is the vector sum of the linear and third-order components. The third-order output can be partitioned into two components: one in the direction of the linear output and the other orthogonal to it. The uncorrelated distortion output can now be identified in terms of a canceling process where a scaled replica of the input signal is subtracted from the total nonlinear output. The orthogonal component cannot be canceled by a scaled replica of the input signal and, hence, it represents the effective uncorrelated distortion that contributes to the degradation of system SINAD performance, while the correlated component of the third-order output represents the correlated distortion that causes gain compression of the linear output. This definition complies with the definition of nonlinear distortion in communication theory [16]–[18] where the effective SNR is calculated as ratio of the effective signal component (which includes the correlated distortion or gain compression) to the effective nonlinear distortion component (which is the uncorrelated distortion). Therefore, the uncorrelated distortion

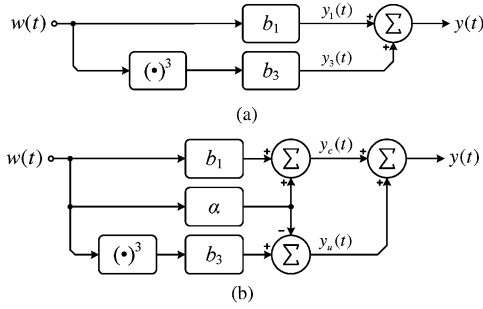


Fig. 2. (a) Instantaneous nonlinear model. (b) Instantaneous nonlinear model with uncorrelated outputs.

noise is treated as an additive noise component similar to the additive white Gaussian noise (AWGN).

In the following, we consider a memoryless nonlinear system, which can be characterized by a power series model:

$$y(t) = \sum_{n=1}^N y_n(t) = \sum_{n=1}^N a_n w^n(t). \quad (1)$$

The power series model represents the instantaneous relationship between the input and output waveforms. In order to identify the orthogonal component of the nonlinear output, we define a canceling signal as a replica of the input signal used to cancel the correlated component of the output

$$w_c(t) = a_1 w(t) + \alpha w(t) \quad (2)$$

where

$$\alpha = \frac{\int_{-\infty}^{\infty} y_3(t) w(t) dt}{\int_{-\infty}^{\infty} w(t)^2 dt} \quad (3)$$

is a cross-correlation coefficient that represents the fraction of the cubic term that is correlated with the linear response. Using this representation, the nonlinear model in (1) depicted in Fig. 2(a), is converted into a model with orthogonal outputs, as shown in Fig. 2(b). Therefore, for a third-order nonlinearity, we define a new set of outputs

$$y_c(t) = a_1 w(t) + \alpha w(t) \quad (4)$$

which is correlated to the input signal and can be canceled by $w_c(t) = y_c(t)$, and

$$y_u(t) = a_3 w(t)^3 - \alpha w(t) \quad (5)$$

which is uncorrelated to the input signal. The new outputs $y_c(t)$ and $y_u(t)$ are orthogonal and represent a useful component and an uncorrelated distortion component and, hence, they define system SINAD.

Now consider a multisine input signal $w(t)$ consisting of the sum of K tones and applied to the nonlinear amplifier so that

$$w(t) = \sum_{k=1}^K w_k(t). \quad (6)$$

Here, the signal $w_k(t)$ is the k th tone with radian frequency ω_k and phase ϕ_k

$$w_k(t) = A_k \cos(\omega_k t + \phi_k). \quad (7)$$

The complex envelope of this signal is equivalent to the phasor form of sinusoids

$$\tilde{w}_k(t) = A_k e^{j\phi_k}. \quad (8)$$

The response of the nonlinear system to a multisine signal consists of all intermodulation products of the input tones. Now using (1) and applying the multisine signal model in (7), the component of $y_n(t)$ centered at frequency $\omega = \omega_{k_1} + \dots + \omega_{k_n}$ due to the intermodulation of input components (centered at the frequency vector $(\omega_{k_1}, \dots, \omega_{k_n})$) can be expressed as [19]

$$\tilde{y}_{n,\omega}(t) = \sum_{\omega_{k_1} + \dots + \omega_{k_n} = \omega} \frac{a_n}{2^{n-1}} \binom{n}{n_{-K}, \dots, n_K} \prod_{i=1}^n A_{k_i} e^{j\phi_{k_i}} \quad (9)$$

where $\omega = \sum_{k=-K}^K n_k \omega_k = \sum_{i=1}^n \omega_{k_i}$, $\sum_{k=-K}^K n_k = n$, and

$$\binom{n}{n_{-K}, \dots, n_K} = \frac{n!}{n_K! \dots n_{-K}!} \quad (10)$$

is the multinomial coefficient. In the following, we consider the special cases of single-, two-, and four-tone signals and we derive the output distortion components by which the effective in-band distortion is identified.

A. Single Tone

Let us first consider the case where the input consists of a single tone of frequency ω_c , therefore,

$$w(t) = A \cos(\omega_c t + \phi) \quad (11)$$

then using (9), the complex envelope of the output at the fundamental frequency ω_c is

$$\tilde{y}(t) = \sum_{n=1}^N b_n \tilde{w}^{* \frac{n-1}{2}} \tilde{w}^{\frac{n+1}{2}} = \sum_{n=1}^N b_n A^n e^{j\phi} \quad (12)$$

where

$$b_n = \frac{a_n}{2^{n-1}} \binom{n-1}{2}, \frac{n+1}{2} \quad (13)$$

are the envelope coefficients and relate the complex envelope of the output to the complex envelope of the input signal [20]. Therefore, the total nonlinear output at the fundamental is

$$y(t) = g_1(A) \cos(\omega_c t + \phi + g_2(A)) \quad (14)$$

where g_1 and g_2 represent the well-known AM–AM and AM–PM characteristics and, thus, the envelope coefficients b_n can be obtained by polynomial fitting of the measured AM–AM and AM–PM characteristics. The nonlinear response to a single tone is, therefore, a replica of the input signal with modified amplitude and phase. A canceling signal in this case can be designed to cancel the whole output and is independent of the initial phase. The output phasor at any of the harmonics can also be derived in compact form in a similar way. Note that the response to a single tone is a single component that is correlated with the input and, hence, in-band distortion is absent. This is intuitive because the response of a nonlinear system to a single tone results in gain compression and not distortion.

B. Two Tone

Now consider a two-tone input with equal amplitudes, then

$$\begin{aligned} w_1(t) &= A \cos(\omega_1 t + \phi_1) \\ w_2(t) &= A \cos(\omega_2 t + \phi_2) \end{aligned} \quad (15)$$

where A is the amplitude and ϕ_i is the phase of each of the input tones. Therefore, using (9) and the proper frequency vectors, the complex envelope of the output at the frequency of the first tone is

$$\tilde{y}_{\omega_1}(t) = \sum_{n=1}^N \sum_{l=0}^{\frac{n-1}{2}} b_{n,l} A^n e^{j\phi_1} \quad (16)$$

and for the second tone is

$$\tilde{y}_{\omega_2}(t) = \sum_{n=1}^N \sum_{l=0}^{\frac{n-1}{2}} b_{n,l} A^n e^{j\phi_2} \quad (17)$$

where $b_{n,l}$ is

$$b_{n,l} = \frac{a_n}{2^{n-1}} \left(l, \frac{n-1}{2} - l, \frac{n+1}{2} - l, l \right). \quad (18)$$

Therefore, the output $y(t)$ at the fundamental frequencies ω_1 and ω_2 can be written as

$$y(t) = g_1(A) \cos[\omega_1 t + \phi_1 + g_2(A)] + g_1(A) \cos[\omega_2 t + \phi_2 + g_2(A)] \quad (19)$$

where $g_1(A)$ and $g_2(A)$ are real functions of the amplitudes and which represent the AM–AM and AM–PM conversions,

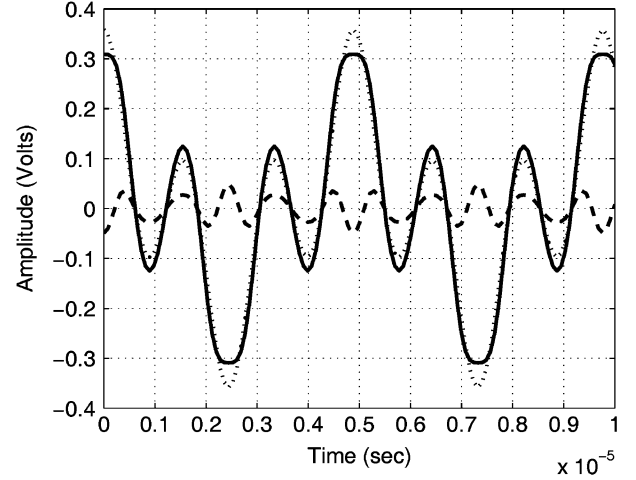


Fig. 3. Time-domain representation of a phase-aligned four-tone signal. Solid: output signal. Dotted: canceling signal. Dashed: in-band distortion.

respectively. Note that with a two-tone signal, the output tones that lie within the input band have the same phase change as the linear output regardless of the initial phase of the input tones and the nonlinear order. Therefore, effective in-band distortion is absent, as considering (19), the output signal has a phase that is totally correlated with the input signal. Thus, a canceling signal can be designed to cancel the output signal at the fundamental frequencies completely regardless of the initial phase.

C. Four Tone

For a four-tone input with each tone having an amplitude A , the input $w(t)$ is

$$w(t) = \sum_{i=1}^4 A \cos(\omega_i t + \phi_i). \quad (20)$$

The derivation of a closed form for the output for orders higher than 3 is more laborious than for the single- and two-tone cases. For illustrative purposes, we consider a third-order nonlinear system (one described by a third-order power series). Using (7), the output complex envelope at the fundamental frequencies is shown in (21) as follows:

$$\begin{aligned} \tilde{y}_{\omega_1}(t) &= b_1 A e^{j\theta_1} + b_3 A^3 \\ &\quad \times \left(7e^{j\theta_1} + e^{j(2\theta_2 - \theta_3)} + 2e^{j(\theta_2 + \theta_3 - \theta_4)} \right) \\ \tilde{y}_{\omega_2}(t) &= b_1 A e^{j\theta_2} + b_3 A^3 \left(7e^{j\theta_2} + e^{j(2\theta_3 - \theta_4)} \right. \\ &\quad \left. + 2e^{j(\theta_4 + \theta_1 - \theta_3)} + 2e^{j(\theta_3 + \theta_1 - \theta_2)} \right) \\ \tilde{y}_{\omega_3}(t) &= b_1 A e^{j\theta_3} + b_3 A^3 \left(7e^{j\theta_3} + e^{j(2\theta_2 - \theta_1)} \right. \\ &\quad \left. + 2e^{j(\theta_4 + \theta_1 - \theta_2)} + 2e^{j(\theta_4 + \theta_2 - \theta_3)} \right) \\ \tilde{y}_{\omega_4}(t) &= b_1 A e^{j\theta_4} + b_3 A^3 \\ &\quad \times \left(7e^{j\theta_4} + e^{j(2\theta_3 - \theta_2)} + 2e^{j(\theta_3 + \theta_2 - \theta_1)} \right) \end{aligned} \quad (21)$$

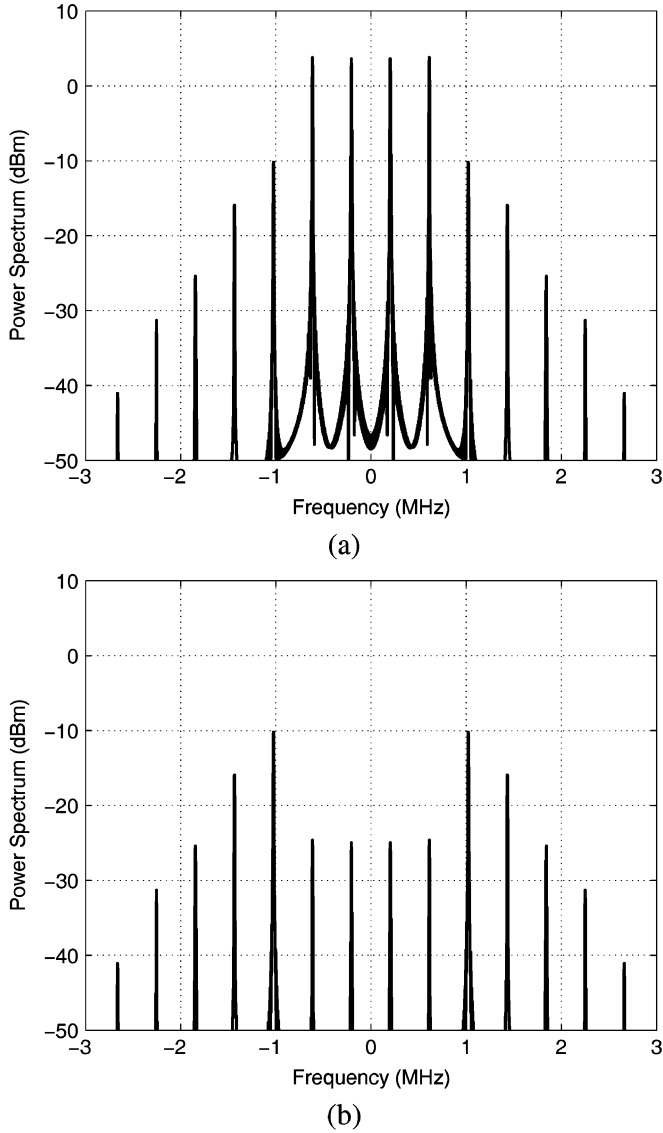


Fig. 4. (a) Output spectrum and (b) uncorrelated distortion spectrum for phase aligned four-tone signal (frequencies are offset from the carrier frequencies).

where $b_1 = a_1$ and $b_3 = (3/4)a_3$. Therefore, the total output at the fundamental angular frequencies $(\omega_1, \dots, \omega_4)$ can then be written as

$$y(t) = \sum_{i=1}^4 g_{1i}(A) \cos(\omega_i t + \Theta_i(\phi_1, \dots, \phi_4) + g_{2i}(A)) \quad (22)$$

where $g_{1i}(A)$ and $g_{2i}(A)$ are real functions of the input amplitudes and the nonlinear coefficients and $\Theta_i(\phi_1, \dots, \phi_4)$ is a linear function of the initial phases ϕ_i . Note that a four-tone signal produces distortion components at the fundamental frequencies that can be either correlated or uncorrelated with the linear output depending on the initial phases of the input tones. The output components at the fundamental frequencies consist of the vector sum of different components and, therefore, depending on phase combinations.

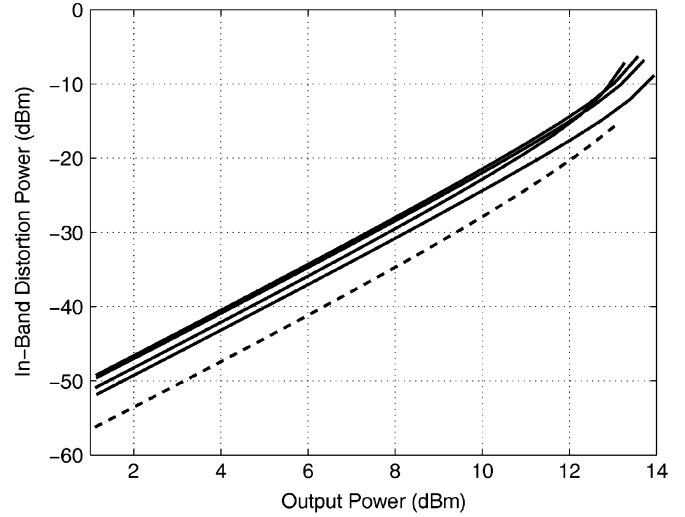


Fig. 5. In-band distortion for different phase combinations of a four-tone signal (solid) and zero initial phase (dashed).

For the special case where the initial phases of the input tones are zero, different terms in each of the output components in (21) add up in the following way:

$$\begin{aligned} \tilde{y}_{\omega_1}(t) &= \tilde{y}_{\omega_4}(t) = B_1 \\ \tilde{y}_{\omega_2}(t) &= \tilde{y}_{\omega_3}(t) = B_2 \end{aligned} \quad (23)$$

where $B_1 = b_1 A + 10b_3 A^3$ and $B_2 = b_1 A + 12b_3 A^3$. Hence, (21) becomes

$$\begin{aligned} y(t) &= |B_1| \cos(\omega_1 t + \angle B_1) + |B_2| \cos(\omega_2 t + \angle B_2) \\ &\quad + |B_2| \cos(\omega_3 t + \angle B_2) + |B_1| \cos(\omega_4 t + \angle B_1) \end{aligned} \quad (24)$$

Note that the amplitude of the output at each of the four tones is not equal and, therefore, a canceling signal will not cancel the whole signal at the fundamental frequencies and, hence, the remainder is in-band distortion. The coefficient α for a four-tone signal can be computed from (3) as

$$\alpha = 11b_3 A^2 \quad (25)$$

and, hence, the in-band distortion component is

$$\begin{aligned} y_{IB}(t) &= y(t) - w_c(t) \\ &= 2b_3 A^3 [\cos(\omega_1 t) - \cos(\omega_2 t) - \cos(\omega_3 t) + \cos(\omega_4 t)]. \end{aligned} \quad (26)$$

Note that the in-band distortion components have equal powers at the four fundamental tones in the case of phase-aligned tones (zero initial phases). The same analysis can be performed when the initial phases are not zero. Fig. 3 shows a time-domain representation of the phase-aligned four-tone signal, a canceling signal, and the resulting in-band distortion. The frequency-domain representation is depicted in Fig. 4 where the total output spectrum and the total uncorrelated distortion spectrum are simulated. Fig. 5 shows the effective in-band distortion of the four-tone signal as a function of input power and for different initial phase combinations. Note that the minimum in-band dis-

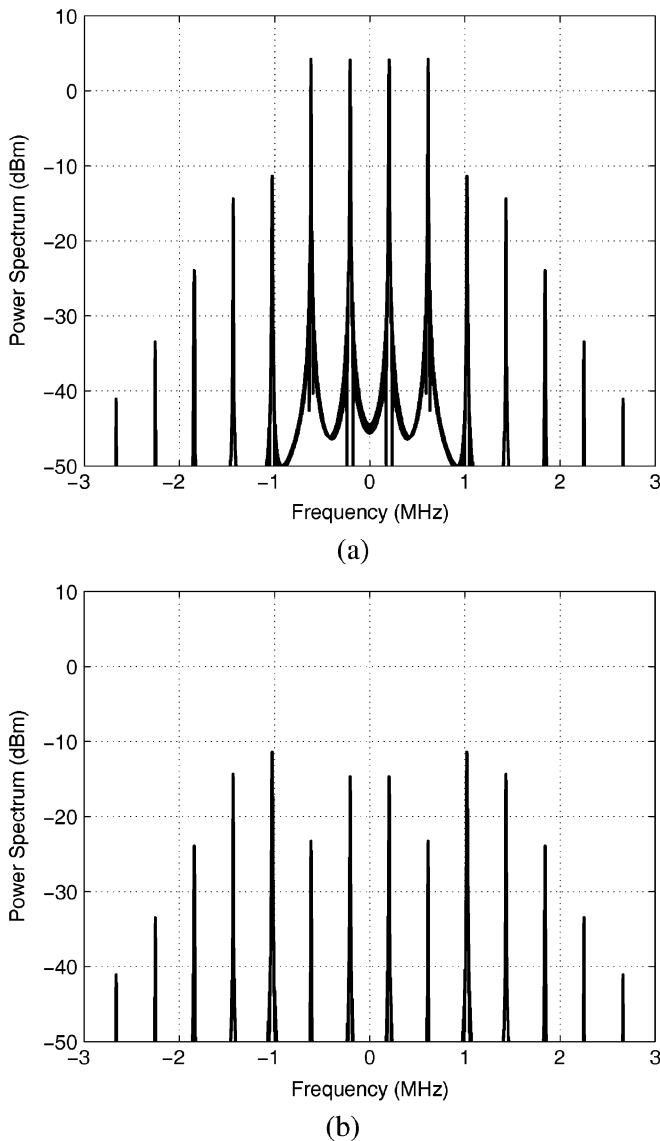


Fig. 6. (a) Output spectrum and (b) uncorrelated distortion spectrum of a four-tone signal with random phase.

tortion occurs when the initial phases are zero (phase aligned multisines).

D. Discussion

The above analysis provides a basis for the identification of effective in-band distortion of multisine signals. However, it is not adequate for identifying distortion when the input tones have random phases and/or amplitudes. Therefore, with random waveforms, the definition of in-band distortion needs a probabilistic model in order to provide a useful description of distortion in terms of signal statistics. A multisine signal with random amplitude and phase resembles a digitally modulated carrier where the signal does not have a deterministic representation. Therefore, multisines are a useful tool in understanding distortion in communication signals. In Section IV, we develop the

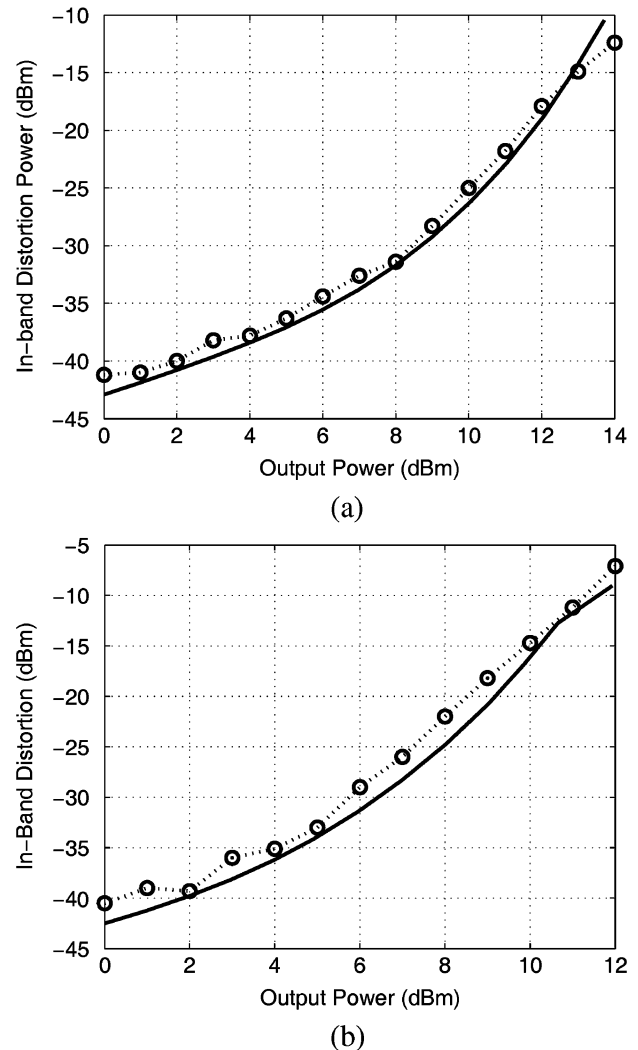


Fig. 7. In-band distortion of phase-aligned: (a) four- and (b) eight-tone signal. \circ : measured. Solid: simulation.

probabilistic view of in-band distortion using the same concepts developed here about the orthogonalization of a behavioral model, but with the probabilistic tools that suit the random nature of signals.

IV. DISTORTION OF MULTISINES WITH RANDOM PHASES

In [3], we presented a statistical analysis of in-band distortion of multisines with random phases. The orthogonalization of the behavioral model with random inputs is a probabilistic version of the one described in Section III for deterministic signals. The analysis of multisines with random phases assumes that multisines have uniformly distributed random phases and, hence, the estimated distortion is found as a statistical average. The statistical average is estimated in simulation by computing the average distortion of a large number of realizations of the multisines having phases generated using a random number generator for each realization, as will be shown in Section V.

The orthogonalization of the behavioral model enables the uncorrelated output distortion to be treated as an additive noise similar to the AWGN and enables the SINAD to be determined since the effective noise-like component of the output nonlinear

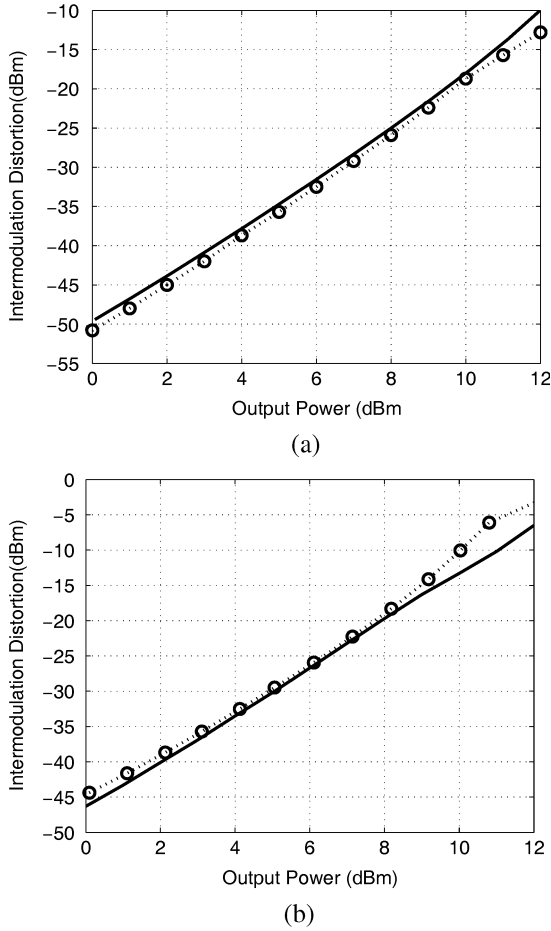


Fig. 8. Intermodulation distortion of phase aligned: (a) four- and (b) eight-tone signal. \circ measured. Solid: simulation.

power is determined. It is worth emphasizing here that the analysis presented in [3] does not require the input signal to have Gaussian distribution, which is a common assumption for a large number of tones with random phases. Therefore, it is valid with any number of tones provided that their phases are completely random.

A complete derivation of the output autocorrelation function of different multisine signals with random phases can be found in [3]. It was shown that the response of the nonlinearity to a single-tone input with random phase is a single tone with a compressed amplitude regardless of the initial phase

$$R_{\tilde{y}_c \tilde{y}_c}(\tau) = |b_1 + b_3 A^2|^2 R_{\tilde{w} \tilde{w}}(\tau). \quad (27)$$

Therefore, the output is completely correlated with the input and, thus, a nonlinear system exhibits gain compression or expansion without generating effective in-band distortion. With two-tone excitation, the output consists of compressed outputs at the fundamental frequencies and uncorrelated out-of-band intermodulation components

$$R_{\tilde{y}_u \tilde{y}_u}(\tau) = \frac{|b_3|^2 A^6}{32} \cos\left(\frac{3\omega_m \tau}{2}\right). \quad (28)$$

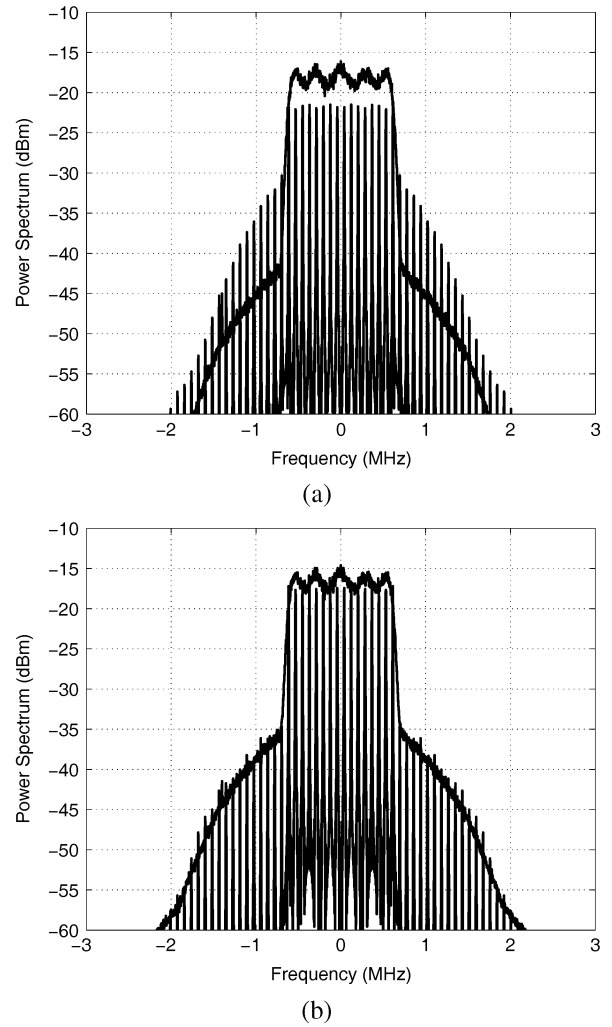


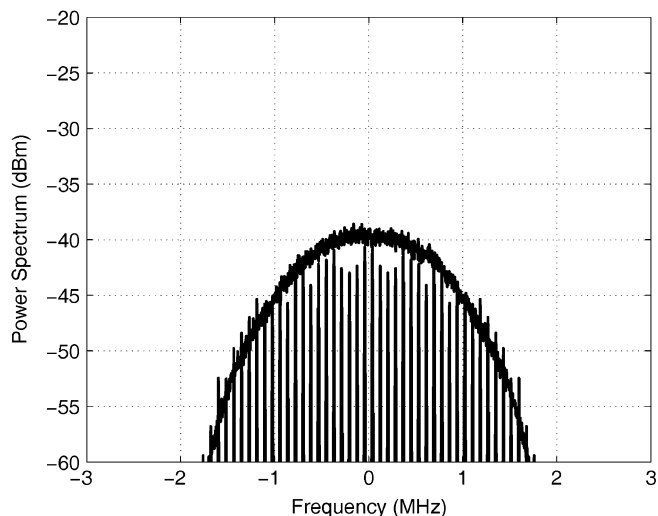
Fig. 9. Simulated output spectrum of 16-tone signal and an IS-95 signal (solid line). (a) Phase aligned tones. (b) Random phases.

Note that a two-tone test does not predict the existence of uncorrelated in-band distortion since the only distortion terms that result as uncorrelated components are the intermodulation components, which lie outside the frequency band of the input tones. Therefore, single- and two-tone tests are inadequate for characterizing in-band uncorrelated distortion.

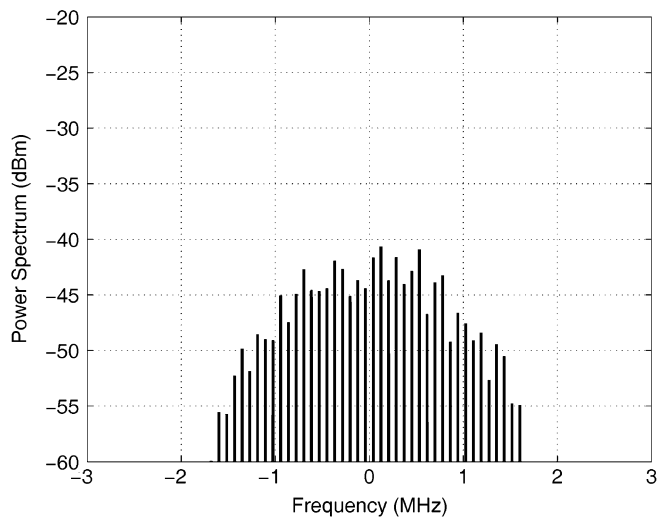
In the case of K tones where $K > 2$, the output distortion consists of uncorrelated in-band components (at the fundamental frequencies) in addition to uncorrelated out-of-band components. In particular, with a four-tone signal with random phases, the amount of in-band distortion is higher than if the phases are aligned, e.g., with zero degree initial phases

$$R_{\tilde{y}_u \tilde{y}_u}(\tau) = \frac{|b_3|^2 A^6}{32} \left[9 \cos\left(\frac{\omega_m \tau}{2}\right) + \cos\left(\frac{3\omega_m \tau}{2}\right) + 18 \cos\left(\frac{5\omega_m \tau}{2}\right) + 9 \cos\left(\frac{7\omega_m \tau}{2}\right) + \cos\left(\frac{9\omega_m \tau}{2}\right) \right]. \quad (29)$$

This is because the output components add to the linear output, whereas with random phases the probability of having components that are orthogonal to the linear output is higher and,



(a)



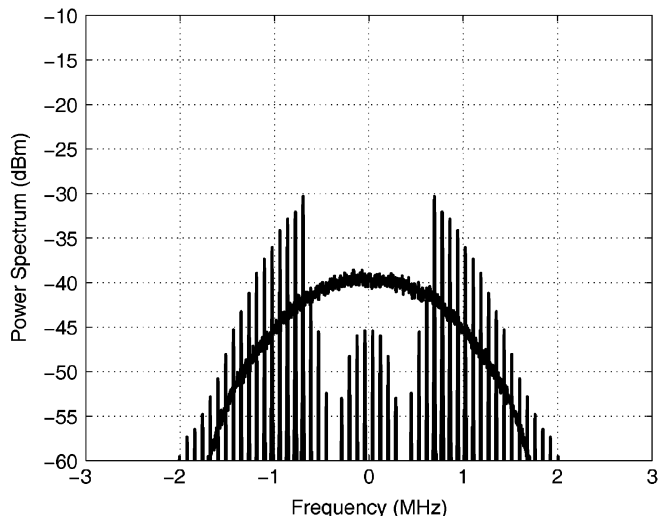
(b)

Fig. 10. Uncorrelated distortion spectrum of random-phase 16-tone signal and an IS-95 signal (solid line). (a) Simulated. (b) Measured.

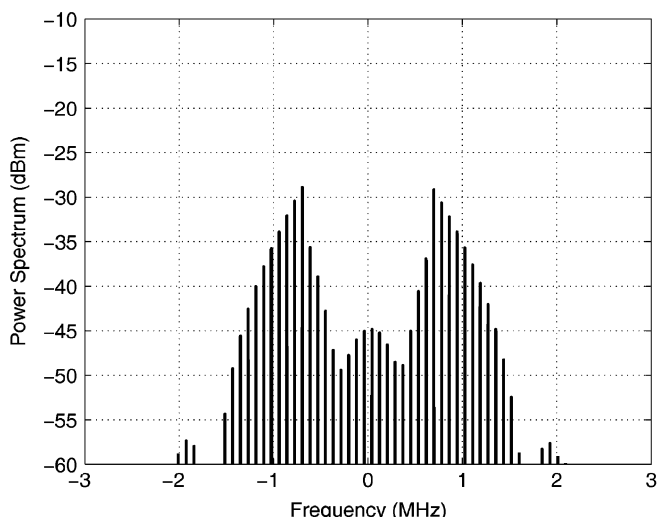
hence, these components are considered as effective in-band distortion. Fig. 6 shows a simulated output spectrum and the uncorrelated distortion spectrum of a four-tone signal with uniformly distributed random phase.

V. MEASUREMENTS AND SIMULATION RESULTS

The analytical evaluation of effective in-band distortion obtained using the orthogonalization procedure was verified by measurements done with multisine signals. The measurements presented here were taken using an Agilent 8510 VNA, E4438C vector signal generator, E4445A spectrum analyzer, and 89600S vector signal analyzer (VSA). The amplifier considered has a gain of 21 dB, an output 1-dB compression point of 11 dBm, and an output third-order intercept (OIP3) of 18 dBm all at 2.0 GHz. The coefficients of the envelope model of the device-under-test were obtained by measuring the AM-AM and AM-PM characteristics at 2 GHz. A polynomial of order 5 was fitted to the complex data using classical least squares polynomial fitting and a set of envelope coefficients (b_n) was obtained. The orthogonal



(a)



(b)

Fig. 11. Uncorrelated distortion spectrum of phase aligned 16-tone signal and an IS-95 signal. (a) Simulated. (b) Measured.

model coefficients were then obtained using the development in Section II.

Multisine signals were generated using an Agilent ESG 4438C vector signal generator. Uncorrelated distortion was obtained using the feed-forward cancellation scheme presented in [15] and the effective in-band distortion was measured within the signal bandwidth using an Agilent VSA. Simulated multisines were generated in MATLAB. The phases of the input tones were randomized using a uniform random number generator. Distortion was estimated by averaging a large number of phase realizations. The number of realizations required depends on the number of tones since, as the number of tones increases, the probability of having a uniformly distributed phases increases. Figs. 7 and 8 show measured and simulated effective in-band and out-of-band distortions of the phase-aligned multisine signals. A good agreement between predicted and simulated values of the in-band and out-of band distortions is shown.

The analysis of multisine signals was used here to estimate distortion of CDMA signals. Nonlinear distortion of multisine

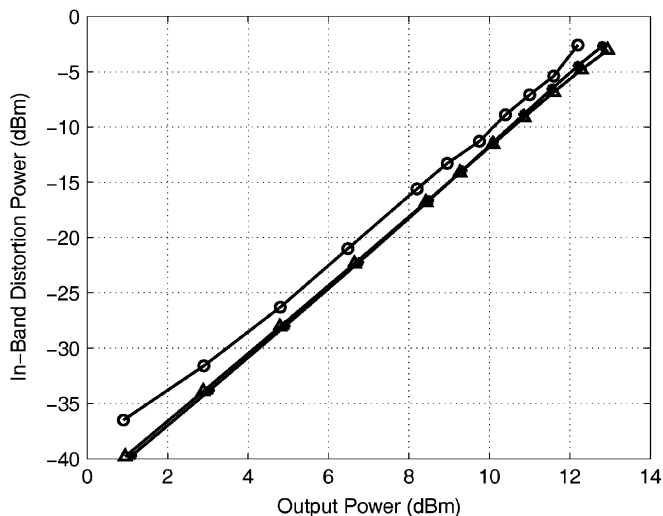


Fig. 12. In-band distortion versus input power. *: simulated random phase 16-tone signal. Δ : simulated CDMA signal. \circ : measured CDMA signal. Solid: simulated phase aligned 16-tone signal.

signals with random phases mimics that of CDMA signals. It was found that distortion of a 16-tone signal with random phases converges to that of a forward-link IS-95 CDMA signal, as shown in Fig. 9(a). This figure shows the output and the uncorrelated distortion spectra of a 16-tone signal with random phases compared to those of a forward-link IS-95 spectrum. The 16-tone signal was designed to have a total bandwidth equal to the bandwidth of an IS-95 CDMA signal (1.2288 MHz) and the tones were equally spaced. A maximum of ten runs for the randomization of the input phases was needed to reach convergence. Fig. 9(b) shows the spectrum of a phased-aligned 16-tone signal compared to that of a CDMA signal. Fig. 10(a) shows the simulated uncorrelated distortion spectrum of a 16-tone signal with random phases compared to that of a forward-link IS-95 signal (the solid line). While Fig. 10(b) shows measured uncorrelated distortion spectrum obtained using feed-forward cancellation. Fig. 11(a) and (b) shows the simulated and measured uncorrelated distortion spectrum of a phase-aligned 16-tone signal compared to that of a forward-link IS-95 signal (solid line).

These figures also show that the shape of the effective in-band spectrum depends on the number of tones and their initial phases. It is clear that in-band distortion is minimum when the phases are aligned, while the out-of-band distortion is at its maximum. The uncorrelated distortion has an almost flat spectrum when the input phases are random. The in-band distortion in this case is at its maximum, while the out-of-band distortion is at its minimum. This is because a multisine signal with random phases approaches a Gaussian distribution, which has a flat spectrum for the uncorrelated distortion, as shown in Section III-D. It is clear that multisines with fixed phases overestimate the out-of-band distortion, while they underestimate in-band distortion of CDMA signals. Fig. 12 shows in-band distortion as a function of input power of multisine signals and a CDMA signal and compared to measured in-band distortion of the CDMA signal. This figure shows good agreement in the estimation of in-band distortion of the random multisine and

CDMA signals and with measured data of a CDMA signal. The measured in-band distortion of fixed and constant phase multisine signals are both in good agreement with the simulated spectrums. The depth of the in-band notches observed at the edge of the signal bandwidth for the simulated fixed phase signal are not as deep for the measured in-band distortion due to the finite delay error in the feed-forward cancellation measurement setup.

VI. CONCLUSION

An analysis of multisine signals in a nonlinear system has been developed. The analysis is used for the estimation of effective in-band distortion of communication signals. Traditional two-tone tests have been shown to be inadequate for the estimation of in-band distortion. It was also shown that multisine signals (four tones and more) with random phases can be used to estimate in-band distortion in real communication signals. This is significant because multisine signals are easier and faster to simulate using harmonic-balance techniques. The accuracy of the simulations using multisine signals depends on the number of tones and the randomization of the initial phases.

ACKNOWLEDGMENT

The authors would like to thank the reviewers for their constructive suggestions and comments.

REFERENCES

- [1] V. Rizzoli, N. Neri, F. Mastri, and A. Lipparini, "A Krylov-subspace technique for the simulation of integrated RF/microwave subsystems driven by digitally modulated carriers," *Int. J. RF Microw. Comput.-Aided Eng.*, vol. 9, no. 6, pp. 490–505, 1999.
- [2] K. Vanhoenacker, T. Dobrowiecki, and J. Schoukens, "Design of multisine excitations to characterize the nonlinear distortions during FRF-measurements," *IEEE Trans. Instrum. Meas.*, vol. 50, no. 5, pp. 1097–1102, Oct. 2001.
- [3] K. M. Gharaibeh, K. G. Gard, and M. B. Steer, "Characterization of in-band distortion in RF front-ends using multisine excitation," in *IEEE Radio Wireless Symp.*, 2006, pp. 487–490.
- [4] K. A. Remley, "Multisine excitation for ACPR measurements," in *IEEE MTT-S Int. Microw. Symp.*, Jun. 2003, pp. 2141–2144.
- [5] J. C. Pedro and N. B. de Carvalho, "On the use of multitone techniques for assessing RF components' intermodulation distortion," *IEEE Trans. Microw. Theory Tech.*, vol. 47, no. 12, pp. 2393–2402, Dec. 1999.
- [6] —, "Evaluating co-channel distortion ratio in microwave power amplifiers," *IEEE Trans. Microw. Theory Tech.*, vol. 49, no. 10, pp. 1777–1784, Oct. 2001.
- [7] —, "Characterizing nonlinear RF circuits for their in-band signal distortion," *IEEE Trans. Instrum. Meas.*, vol. 51, no. 3, pp. 420–426, Jun. 2003.
- [8] N. Boulejfjen, A. Harguem, and F. M. Ghannouchi, "New closed-form expression for the prediction of multitone intermodulation distortion in fifth-order nonlinear RF circuits/systems," *IEEE Trans. Microw. Theory Tech.*, vol. 52, no. 1, pp. 121–132, Jan. 2004.
- [9] S. Boyd, "Multitone signals with low crest factor," *IEEE Trans. Circuit Syst.*, vol. CAS-33, no. 10, pp. 1018–1022, Oct. 1986.
- [10] M. Friese, "Multitone signals with low crest factor," *IEEE Trans. Commun.*, vol. 45, no. 10, pp. 1338–1344, Oct. 1997.
- [11] J. F. Sevic and M. B. Steer, "On the significance of envelope peak-to-average ratio for estimating the spectral regrowth of an RF/microwave power amplifier," *IEEE Trans. Microw. Theory Tech.*, vol. 48, no. 6, pp. 1068–1071, Jun. 2000.
- [12] A. Geens, Y. Rolain, W. Van Moer, K. Vanhoenacker, and J. Schoukens, "Discussion on fundamental issues of NPR measurements," *IEEE Trans. Instr. Meas.*, vol. 52, no. 2, pp. 197–202, Feb. 2003.
- [13] N. Blachman, "The signal \times signal, noise \times noise, and signal \times noise output of a nonlinearity," *IEEE Trans. Inf. Theory*, vol. IT-14, no. 1, pp. 21–27, Jan. 1968.

- [14] N. Blachman, "The uncorrelated output components of a nonlinearity," *IEEE Trans. Inf. Theory*, vol. IT-14, no. 3, pp. 250–255, Mar. 1968.
- [15] K. M. Gharaibeh, K. G. Gard, and M. B. Steer, "Estimation of in-band distortion in digital communication system," in *IEEE MTT-S Int. Microwave Symp. Dig.*, Jun. 2005, pp. 1963–1966.
- [16] P. Banelli and S. Cacopardi, "Theoretical analysis and performance of OFDM signals in nonlinear AWGN channels," *IEEE Trans. Commun.*, vol. 48, no. 3, pp. 430–441, Mar. 2000.
- [17] A. Conti, D. Dardari, and V. Tralli, "An analytical framework for CDMA systems with a nonlinear amplifier and AWGN," *IEEE Trans. Commun.*, vol. 50, no. 7, pp. 1110–1120, Jul. 2002.
- [18] M. Eslami and H. Shafiee, "Performance of OFDM receivers in presence of nonlinear power amplifiers," in *Int. Comm. Syst. Conf.*, Nov. 2002, vol. 1, pp. 25–28.
- [19] J. W. Graham and L. Ehrmen, *Nonlinear System Modeling and Analysis with Application to Communication Receivers*. Rome, NY: Rome Air Develop. Ctr., Jun. 1973.
- [20] K. Gard, H. Gutierrez, and M. B. Steer, "Characterization of spectral regrowth in microwave amplifiers based on the nonlinear transformation of a complex Gaussian process," *IEEE Trans. Microw. Theory Tech.*, vol. 47, no. 7, pp. 1059–1069, Jul. 1999.
- [21] K. M. Gharaibeh, K. Gard, and M. B. Steer, "The impact of nonlinear amplification on the performance of CDMA systems," in *IEEE Radio Wireless Conf.*, 2004, pp. 83–86.



Khaled M. Gharaibeh (S'01–M'04) received the B.S. and M.S. degrees in electrical engineering from the Jordan University of Science and Technology, Irbid, Jordan, in 1995 and 1998 respectively, and the Ph.D. degree in electrical engineering from North Carolina State University, Raleigh, in 2004.

From 1996 to 2000, he was a Planning Engineer with Jordan Telecom, Amman, Jordan. From January 2004 to January 2005, he was a Post-Doctoral Research Associate with the Department Electrical and Computer Engineering, North Carolina State University.

He is currently an Assistant Professor of electrical engineering with the Hijawi Faculty for Engineering Technology, Yarmouk University, Irbid, Jordan. His research interests are nonlinear system identification, behavioral modeling of nonlinear RF circuits, and wireless communications.

Dr. Gharaibeh is a member of Eta Kappa Nu.



Kevin G. Gard (S'92–M'95) received the B.S. and M.S. degrees in electrical engineering from North Carolina State University, Raleigh, in 1994 and 1995, respectively, and the Ph.D. degree in electrical engineering from the University of California at San Diego, La Jolla, in 2003.

He is currently the William J. Pratt Assistant Professor with the Electrical and Computer Engineering Department, North Carolina State University. From 1996 to 2003, he was with Qualcomm Inc., San Diego, CA, where he was a Staff Engineer and

Manager responsible for the design and development of RF integrated circuits (RFICs) for code-division multiple-access (CDMA) wireless products. He has designed SiGe BiCMOS, Si BiCMOS, and GaAs metal–semiconductor field-effect transistor (MESFET) integrated circuits for cellular and personal communication systems (PCSs) CDMA, wideband code-division multiple-access (WCDMA), and AMPS transmitter applications. His research interests are in the areas of integrated circuit design for wireless applications and analysis and modeling of nonlinear microwave circuits with digitally modulated signals.

Dr. Gard is a member of the IEEE Microwave Theory and Techniques and Solid-State Circuits Societies, Sigma Xi, Eta Kappa Nu, and Tau Beta Pi.



Michael B. Steer (S'76–M'82–SM'90–F'99) received the B.E. and Ph.D. degrees in electrical engineering from the University of Queensland, Brisbane, Australia, in 1976 and 1983, respectively.

He is currently the Lampe Family Distinguished Professor of Electrical and Computer Engineering, North Carolina State University, Raleigh. In 1999 and 2000, he was a Professor with the School of Electronic and Electrical Engineering, The University of Leeds, where he held the Chair in microwave and millimeter-wave electronics. He was also Director of

the Institute of Microwaves and Photonics, The University of Leeds. He has authored over 300 publications on topics related to RF, microwave and millimeter-wave systems, high-speed digital design, and RF and microwave design methodology and circuit simulation. He coauthored *Foundations of Interconnect and Microstrip Design* (Wiley, 2000).

Prof. Steer is active in the IEEE Microwave Theory and Techniques Society (IEEE MTT-S). In 1997, he was secretary of the IEEE MTT-S. From 1998 to 2000, he was an elected member of its Administrative Committee. He was the Editor-in-Chief of the IEEE TRANSACTIONS ON MICROWAVE THEORY AND TECHNIQUES (2003–2006). He was a 1987 Presidential Young Investigator (USA). In 1994 and 1996, he was the recipient of the Bronze Medallion presented by the Army Research Office for "Outstanding Scientific Accomplishment." He was also the recipient of the 2003 Alcoa Foundation Distinguished Research Award presented by North Carolina State University.